X-692-70-60
PREPRINT

NASA TM X- 63843

OBSERVATIONS OF THE LUNAR MACH CONE

Y. C. WHANG
N. F. NESS

JANUARY 1970

GSFC

GODDARD SPACE FLIGHT CENTER
GREENBELT, MARYLAND

X-692-70-60

OBSERVATIONS OF THE LUNAR MACH CONE

Y.C. Whang

Department of Space Science and Applied Physics
The Catholic University of America
Washington, D.C. 20017

and

N.F. Ness

Laboratory for Extraterrestrial Physics
NASA-Goddard Space Flight Center
Greenbelt, Maryland 20771

January 1970

ABSTRACT

According to Whang's theoretical model, the region of penumbral decreases of the magnetic field in the lunar wake is bounded on its exterior by a Mach cone tangential to the lunar body. The existence of such a lunar Mach cone has been confirmed by NASA-GSFC magnetometer data from lunar Explorer 35. The axis of the Mach cone indicates that the direction of the solar wind comes from $\sim 4.5^{\circ}$ west of the sun as viewed from the moon. With the direct measurements of the solar wind speed, this indicates that the azimuthal velocity is ~ 5 km/sec in the sense of the solar rotation. Due to the variability of the magnetic field direction, the spacecraft has actually observed the three-dimensional wake region of the interaction of the solar wind with the moon. The lack of axial symmetry of the observed lunar Mach cone provides the first experimental evidence for the anisotropic propagation of magnetoacoustic waves in the solar wind. The average Mach angle is found to be $\sim 8^{\circ}$ in directions perpendicular to the magnetic field vector, and $\sim 5.5^{\circ}$ in the direction parallel to the field leading to a velocity anisotropy of ~ 1.4. This compares favorably with the nominal expected value in the solar wind of ~ 1.6, assuming $\beta = 1$ and $T_{\parallel}/T_{\perp} = 1.5$.

INTRODUCTION

In previous publications [Ness et al., 1967; 1968; Taylor et al., 1968; Ogilvie and Ness, 1969; Ness and Schatten, 1969] various results of the NASA-GSFC magnetic field experiment on lunar Explorer 35 were reported. This paper will report the observation of the lunar Mach cone from the same experiment, and discuss its significance as related to the solar wind flow.

When the moon is outside the earth's bow shock, the important features of the observed magnetic field perturbations in the lunar wake include (i) the umbral increase of the magnetic field in the core region of the lunar wake, [See above publications and Colburn et al., 1967], (ii) the penumbral decrease of the magnetic field in the region around the umbral increase, and (iii) the penumbral increase, additional small increases in the field magnitude sometimes observed outside the penumbral decrease.

A recent theoretical study of the solar wind interaction with the moon based on the guiding-center model [Whang, 1968; 1969; 1970] predicted that (i) the principal perturbations of the magnetic field in the lunar wake (the umbral increase and the penumbral decrease) are confined to a region bounded by a Mach cone tangential to the lunar body, and (ii) the penumbral increases occur outside the lunar Mach cone. A summary of these theoretical results is shown in Figure 1. According to

(Figure 1)

this theory, the observation of a change in the lunar wake magnetic signature from a penumbral increase (or from the unperturbed interplanetary condition) to a penumbral decrease is interpreted as the entrance of the spacecraft into the lunar Mach cone. The observation of a change in magnetic signature in a reverse sequence is interpreted as the exit of the spacecraft from the lunar Mach cone. Thus from a fully developed lunar wake magnetic signature, one can determine the time and the position where the spacecraft trajectory intersects the lunar Mach cone.

(Figure 2)

Two lunar wake magnetic signatures are shown in Figure 2 as examples to illustrate the observed crossings of the lunar Mach cone. On April 24, 1968, the spacecraft observed a change in the magnetic signature at 1827 UT from a penumbral increase to a decrease, and another change at 1912 UT from a penumbral decrease to the unperturbed interplanetary condition. The lower half of Figure 2 displays two more crossings of the lunar Mach cone respectively at 1526 UT and 1617 UT on June 15, 1968. More than one hundred clear crossings of the lunar Mach cone were found during the first twelve months of spacecraft operation from July 1967 to July 1968. These crossings are used in this paper to study the geometry of the lunar Mach cone.

MAGNETOACOUSTIC WAVES AND MACH ANGLES

In a collisionless anisotropic plasma, magnetoacoustic waves propagate along the field direction at a speed

$$a = \left[(P_\perp - P_\parallel + B^2/4\pi)/\rho\right]^{1/2}, \tag{1}$$

and in directions perpendicular to the magnetic field at a speed

$$b = \left[(2P_\perp + B^2/4\pi)/\rho\right]^{1/2}, \tag{2}$$

[Lüst , 1959; Whang, 1970]. The velocity anisotropy is

$$\frac{b}{a} = \left[\frac{2 + 2\beta}{2 - \beta(T_\parallel/T_\perp - 1)}\right]^{1/2}, \tag{3}$$

where $T_\parallel/T_\perp$ is the plasma anisotropy, and β the ratio of the perpendicular thermal pressure to the field pressure (the plasma thermal pressure includes both the ion and the electron thermal pressure). The velocity anisotropy as functions of β and $T_\parallel/T_\perp$ are plotted in Figure 3. Assuming $\beta = 1$ and $T_\parallel/T_\perp = 1.5$, the expected velocity anisotropy is ~ 1.6.

(Figure 3)

Because of the anisotropic propagation of magnetoacoustic waves, the lunar Mach cone is not expected to be a right circular one. The axis of the lunar Mach cone indicates the direction of the solar wind velocity $\underset{\sim}{U_o}$. The Mach angle α which is the angle between the axis of the Mach cone and the

generating line varies depending on the position of the generator. The Mach angle in each position is related to the propagation of magnetoacoustic waves in a particular direction with reference to the magnetic field. Let Ψ denote the angle between the wave propagation direction and the field line, then

$$\alpha = \alpha(\Psi). \tag{4}$$

Whang [1970] has calculated the Mach angle for various combinations of the solar wind parameters as a function of the direction angle of the magnetic field. The Mach angles corresponding to the perpendicular and the parallel magnetoacoustic velocity are respectively

$$\alpha_{\perp} = \alpha(\Psi = \pi/2) \approx \sin^{-1}(b/U_0) \tag{5}$$

and

$$\alpha_{\parallel} = \alpha(\Psi = 0) \approx \sin^{-1}(a/U_0) \tag{6}$$

Thus, the velocity anisotropy of magnetoacoustic waves can be approximated by

$$\frac{b}{a} \approx \frac{\sin \alpha_{\perp}}{\sin \alpha_{\parallel}} \tag{7}$$

In this paper experimental data on the observed crossings of the lunar Mach cone are used to deduce the Mach angle α as function of the varying propagation angle Ψ .

Michel (1968) also has suggested the anisotropic propagation of the rarefaction wave in the lunar wake. He considered that the wave propagates

along the field direction with the "acoustic speed" V_s, and perpendicular to the field direction with the "magnetoacoustic speed" V_{MA}. The ratio of V_{MA} to V_s as a function of β for

$$V_s = (\gamma p/\rho)^{1/2}, \tag{8}$$

$$V_{MA} = \left[(\gamma p + B^2/4\pi)/\rho\right]^{1/2}, \tag{9}$$

and $\gamma = 5/3$ is also plotted in Figure 3 to compare it with the velocity anisotropy calculated from Equations (1)-(3).

OBSERVED LUNAR MACH CONE

The first part of this research is to confirm that the observed principal perturbations of the magnetic field are indeed confined to a region bounded by a lunar Mach cone. 28 crossings of the lunar Mach cone corresponding to propagation angle of $\sim 90^\circ$ which were selected for this study are shown in Figure 4. The region of observed penumbral increases and that of penumbral decreases are clearly divided by a Mach cone tangential to the lunar body.

(Figure 4)

The average $\alpha_\perp$ for the 28 crossings is $\sim 8^\circ$ with the axis of the Mach cone making an angle of $\sim 4.5^\circ$ with the Sun-Moon line. The rms deviation of $\alpha_\perp$ is 1.4°. The orbital plane of the Explorer 35 spacecraft is very close to the solar ecliptic plane. Thus during these 28 crossings of the lunar Mach cone the average direction of the solar wind appears to be $\sim 4.5^\circ$ west, as viewed from the moon.

(Figure 5)

If the speed of the solar wind is known, one can calculate the azimuthal velocity of the solar wind. From the MIT Explorer 35 plasma data, [Bridge and Binsack, Private communication] the average speed of the solar wind is measured to be 434 km/sec with an rms deviation of 66 km/sec for the above 28 Mach cone crossings. Based on this speed, the

calculated azimuthal velocity of the solar wind is ~5 km/sec in the direction of the solar rotation as shown in Figure 5. In this simple calculation of the azimuthal velocity, the dependence of the solar wind direction on its speed and the magnetic field vector is not taken into account. The azimuthal velocity calculated from the observed lunar Mach cone seems to be less than that of ~9 km/sec obtained from observations of comet tails (Brandt, 1967) and that of ~10 km/sec obtained directly from the Vela satellites (Hundhausen, 1968).

ANISOTROPIC PROPAGATION OF MAGNETOACOUSTIC WAVES

Experimental data from Explorer 35 spacecraft have been generally analyzed with reference to selenocentric solar ecliptic coordinates (the X_{SSE}-axis parallel to the Moon-Sun line, and Z_{SSE}-axis perpendicular to the to the ecliptic plane). However, as the solar wind interacts with the moon, the perturbed magnetic field and plasma flow in the interaction region are symmetrical about a plane passing through the center of the moon and parallel to the unperturbed magnetic field $\underline{B}_o$ and the unperturbed flow velocity $\underline{U}_o$. Thus, descriptions of field and plasma with reference to a coordinate system related to this symmetry plane can best characterize the real interaction between the solar wind and the moon. For this purpose a new coordinate system is introduced herein with the XY-plane coinciding with the plane of symmetry and the X-axis parallel to $\underline{U}_o$, which is assumed to be 4.5° west as referenced to the Sun-Moon line on the ecliptic plane.

An example of the spacecraft trajectory on April 24, 1968 is shown in Figure 6 in the two different coordinate systems. The upper half of the figure

(Figure 6)

shows that the orbital plane of the spacecraft is close to the ecliptic plane. Because of the variability of the magnetic field direction, especially the solar ecliptic latitude, the inclination of the orbital plane with respect to the plane of symmetry varies considerably. The lower half of figure 6 shows that in the

new coordinate system, the spacecraft trajectories are no longer confined to the region near a plane. Thus, the experimental data from Explorer 35 can be used to describe the three-dimensional wake region of the interaction of the solar wind with the moon.

The next part of this paper presents experimental evidences for the anisotropic propagation of the magnetoacoustic waves in the solar wind.

Let (X, Y, Z) denote the location of an observed Mach cone crossing with reference to the new coordinate system. The Mach angle α associated with the observed Mach cone crossing can be approximately calculated from

$$\tan\alpha = \frac{(Y^2 + Z^2)^{1/2} - 1}{X} \tag{10}$$

Choosing $\alpha^* = 8^\circ$ as a reference Mach angle, a normalized magnetoacoustic speed can be defined as

$$C = \sin\alpha/\sin\alpha^* \tag{11}$$

For the purpose of calculating the angle of propagation, Ψ, let ϕ_o denote the direction angle of the unperturbed magnetic field (the angle between $-\underline{U}_o$ and $\underline{B}_o$) and

$$\theta = \tan^{-1}(Z/Y). \tag{12}$$

Then one can obtain

$$\cos\Psi \approx \cos\theta\sin\phi_o. \tag{13}$$

An elliptical relationship betwen C and Ψ is expected for the anisotropic propagation of magnetoacoustic waves.

(Figure 7)

116 observed crossings of the lunar Mach cone are available for study. The values of C and Ψ calculated from these crossings are plotted in Figure 7. The experimental data are divided into 5 subsets to show that the average value of C is an increasing function of Ψ. For $75^\circ < \Psi < 90^\circ$ the average value of C is 0.98, and the average Mach angle $\alpha = 7.8^\circ$. For $30^\circ < \Psi < 45^\circ$ the average value of C is 0.78, and the average Mach angle is 6.2°. The rms deviation of C is 0.17. The relationship between C and Ψ can be approximated by an ellipse with the ratio of the two axes ~ 1.4. Thus the observed velocity anisotropy of the magnetoacoustic wave is ~ 1.4 and the Mach angle corresponding to zero propagation angle, $\alpha_{\parallel} \sim 5.5^\circ$.

Only 2 clear crossings of the lunar Mach cone (2 percent of the total 116 crossings) were found for $\Psi < 30^\circ$. One has $\phi_o = 89.5^\circ$ and $\theta = 20.3^\circ$, and the other has $\phi_o = 67.2^\circ$ and $\theta = 10.5^\circ$. Small values of Ψ mean that both $\sin \phi_o$ and $\cos \theta$ are near to unity. When the field is nearly perpendicular to the solar wind direction, perturbations of the magnetic field are small near the plane of symmetry. Thus when Ψ is small, perturbations of the magnetic field are small near the crossings of the lunar Mach cone. It becomes difficult to identify the crossings from the magnetic signatures under these conditions.

SUMMARY

In supersonic aerodynamics, when a gas flows past a thin airfoil, the leading edge of the disturbed region should cut across the streamlines upstream at a Mach angle. On this basis Siscoe et al. [1969] found that if the leading edge of the disturbed region in the lunar wake is attached to the lunar body, the measured Mach angles are at least twice the expected Mach angle of the solar wind. This result led them to infer the existence of an "effective lunar profile" which deflects the solar wind flow away from the moon to form a detached lunar compression wave.

Our interpretation of the lunar Mach cone is based on Whang's theory [1969, 1970] which assumes that the moon absorbs all charged particles that impact its surface. Thus, the solar wind flow cannot be deflected by the lunar surface as in an ordinary continuum flow. He suggested that the penumbral increases of the magnetic field and the plasma density should occur outside of the Mach cone attached to the lunar body. This theory is found to be completely consistent with our present experimental observations of the lunar Mach cone.

Due to the variability of the magnetic field direction, the spacecraft has actually observed the three-dimensional interaction of the solar wind with the moon with reference to a new coordinate system (with one of its coordinate axes coinciding with $\underset{\sim}{U}_o$ and another axis parallel to vector $\underset{\sim}{U}_o \times \underset{\sim}{B}_o$). Experimental data on the observed lunar Mach cone are used to deduce the elliptical relationship between the magnetoacoustic velocity and the propagation angle. These observations

provide the first experimental evidence for the anisotropic propagation of magnetoacoustic waves in the solar wind. The ratio of the magnetoacoustic velocities b/a is ~ 1.4. The average Mach angle is $\alpha_{\perp} \sim 8^{\circ}$ in directions perpendicular to the magnetic field, and $\alpha_{\parallel} \sim 5.5^{\circ}$ in the direction parallel to the field.

ACKNOWLEDGMENTS

We are indebted to Dr. L.F. Burlaga for many helpful discussions about this problem. The plasma data used herein were kindly made available by Drs. H.S. Bridge and J.H. Binsack.

The work at the Catholic University of America was supported by the National Aeronautics and Space Administration under Grant NGR-09-005-063.

REFERENCES

Brandt, J.C., Gross plasma velocities from the orientations of ionic comet tails, Astrophys. J., 147, 201, 1967.

Colburn, D.S., R.G. Currie, J.D. Mihalov, and C.P. Sonnett, Diamagnetic solar-wind cavity discovered behind the moon, Science, 158, 1040, 1967.

Hundhausen, A.J., Direct observations of solar wind particles, Space Sci. Rev., 8, 690, 1968.

Lüst, V.R., Über die Ausbreitung von Wellen in einem Plasma, Fortschritte der Physik, 7, 503, 1959.

Michel, F.C., Magnetic field structure behind the moon, J. Geophysic. Res., 73, 1533, 1968.

Ness, N.F., K.W. Behannon, C.S. Scearce and S.C. Cantarano, Early results from the magnetic field experiment on lunar Explorer 35, J. Gephysics Res., 72, 5769, 1967.

Ness, N.F., K.W. Behannon, H.E. Taylor and Y.C. Whang, Perturbations of the interplanetary magnetic field by the lunar wake, J. Geophysics Res., 73, 3421, 1968.

Ness, N.F. and K.H. Schatten, Detection of interplanetary magnetic field fluctuations stimulated by the lunar wake, J. Geophys. Res., 74, 6425, 1969.

Ogilvie, K.W. and N.F. Ness, Dependence of the lunar wake on solar wind plasma characteristics, J. Geophys. Res., 74, 4123, 1969.

Siscoe, G.L., E.F. Lyon, J.H. Binsack and H.S. Bridge, Experimental evidence for a detached lunar compression wave, J. Geophys. Res., 74, 59, 1969.

Taylor, H.E., K.W. Behannon and N.F. Ness, Measurements of the perturbed-interplanetary magnetic field in the lunar wake, J. Geophys. Res., 73, 6723, 1968.

Whang, Y.C., Interaction of the magnetized solar wind with the moon, Phys. of Fluids, 11, 969, 1968.

Whang, Y.C., Field and plasma in the lunar wake, Phys. Rev., 186, 143, 1969.

Whang, Y.C., Two-dimensional guiding-center model for the solar wind-moon interaction, Submitted to J. Geophys. Res. for publication, 1970.

FIGURE CAPTIONS

Fig. 1 According to the theoretical result of Whang's guiding-center model, the region of penumbral decrease of the magnetic field in the lunar wake is bounded on the exterior by a Mach cone tangential to the lunar body. When the spacecraft enters or leaves the region of penumbral decreases, a crossing of the lunar Mach cone is observed.

Fig. 2 The two lunar wake magnetic signatures illustrates the observed crossings of the lunar Mach cone. The upper magnetic signature displays two crossings of the Mach cone at 1827 UT and 1912 UT on April 24, 1968. The lower one displays two crossings at 1526 UT and 1617 UT on June 15, 1968.

Fig. 3 The velocity anisotropy of the magnetoacoustic wave b/a as a function of β and $T_{\parallel}/T_{\perp}$.

Fig. 4 A clear lunar Mach cone is observed. The average Mach angle $\alpha_{\perp}$ is $\sim 8^{\circ}$ in directions perpendicular to the magnetic field vector. The center line of the Mach cone indicates that the average direction of the solar wind is $\sim 4.5^{\circ}$ west as viewed from the moon.

Fig. 5 For the 28 crossings of the lunar Mach cone shown in Fig. 4, the average direction of the solar wind is $\sim 4.5^{\circ}$ west, the average solar wind speed is 434 km/sec. Thus the average azimuthal velocity is $\sim$ 5 km/sec in the direction of the solar rotation.

Fig. 6 In a selenocentric solar ecliptic coordinate, the spacecraft trajectories are confined to the region close to the ecliptic plane. Due to the variability of the magnetic field direction, the spacecraft has actually observed the three-dimensional interaction of the solar wind with the moon with reference to a transformed coordinate system.

Fig. 7 Experimental data on the crossings of the lunar Mach cone are used to deduce the elliptical relationship between the magnetoacoustic velocity and the propagation angle. These observations provide the evidence for the anisotropic propagation of the magnetoacoustic waves in the solar wind.

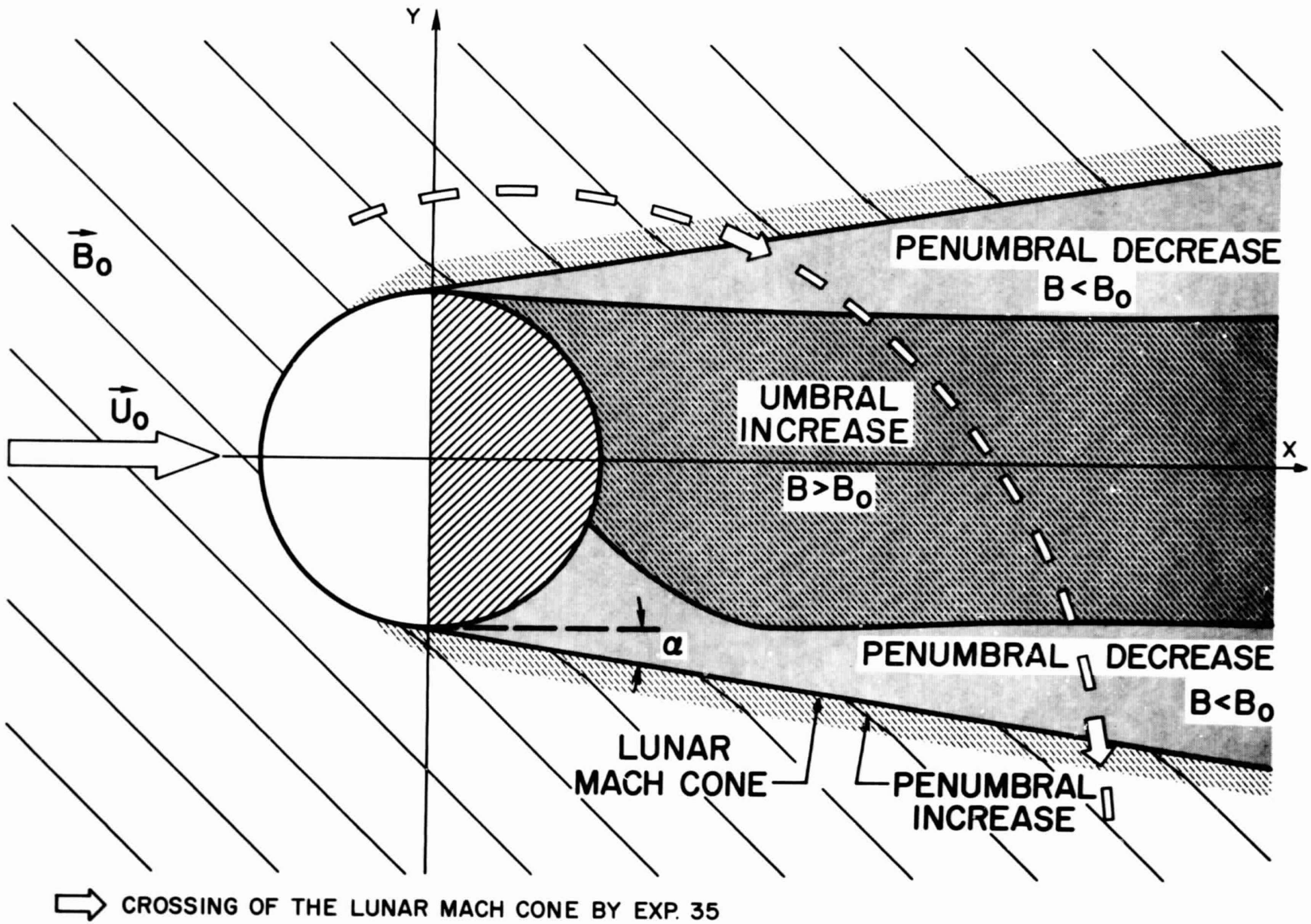
Y
X
$\vec{B}_0$
$\vec{U}_0$
PENUMBRAL DECREASE
$B < B_0$
UMBRAL
INCREASE
$B > B_0$
PENUMBRAL DECREASE
$B < B_0$
α
LUNAR
MACH CONE
PENUMBRAL
INCREASE
CROSSING OF THE LUNAR MACH CONE BY EXP. 35

Fig. 1

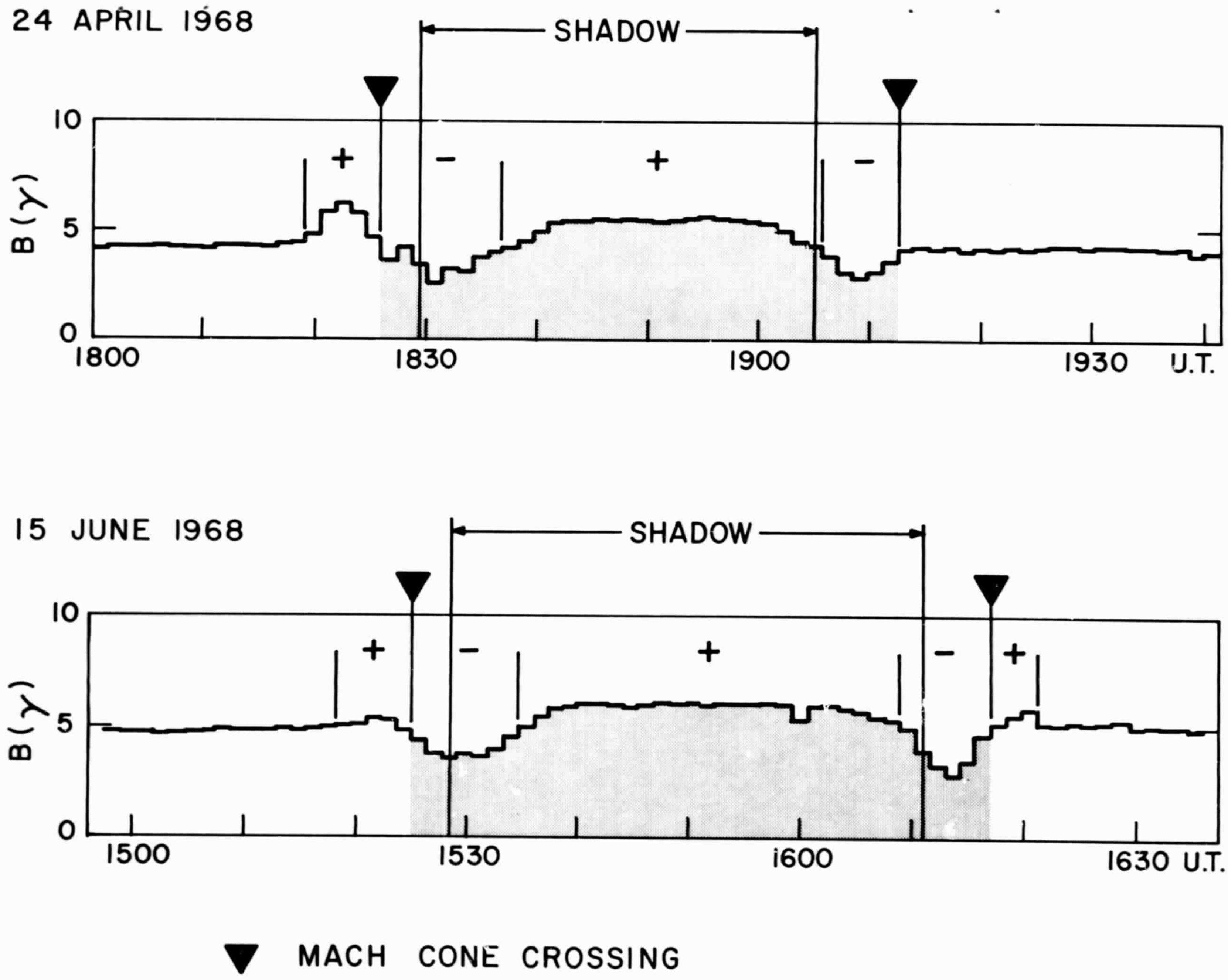
24 APRIL 1968
SHADOW
+
-
+
-
10
5
0
B (γ)
1800
1830
1900
1930
U.T.
15 JUNE 1968
SHADOW
+
-
+
-
+
10
5
0
B (γ)
1500
1530
1600
1630 U.T.
MACH CONE CROSSING

Fig. 2

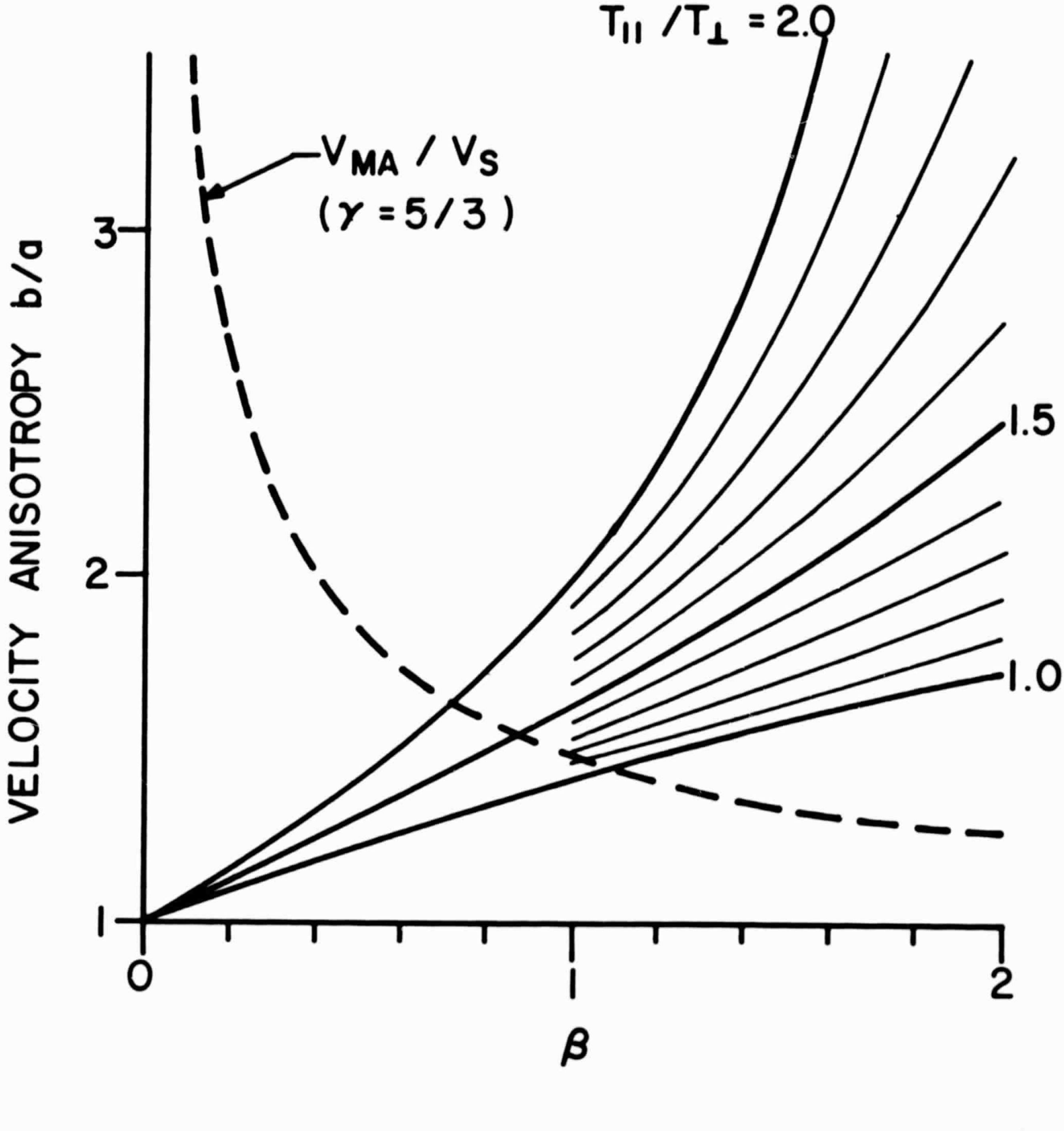

Fig. 3

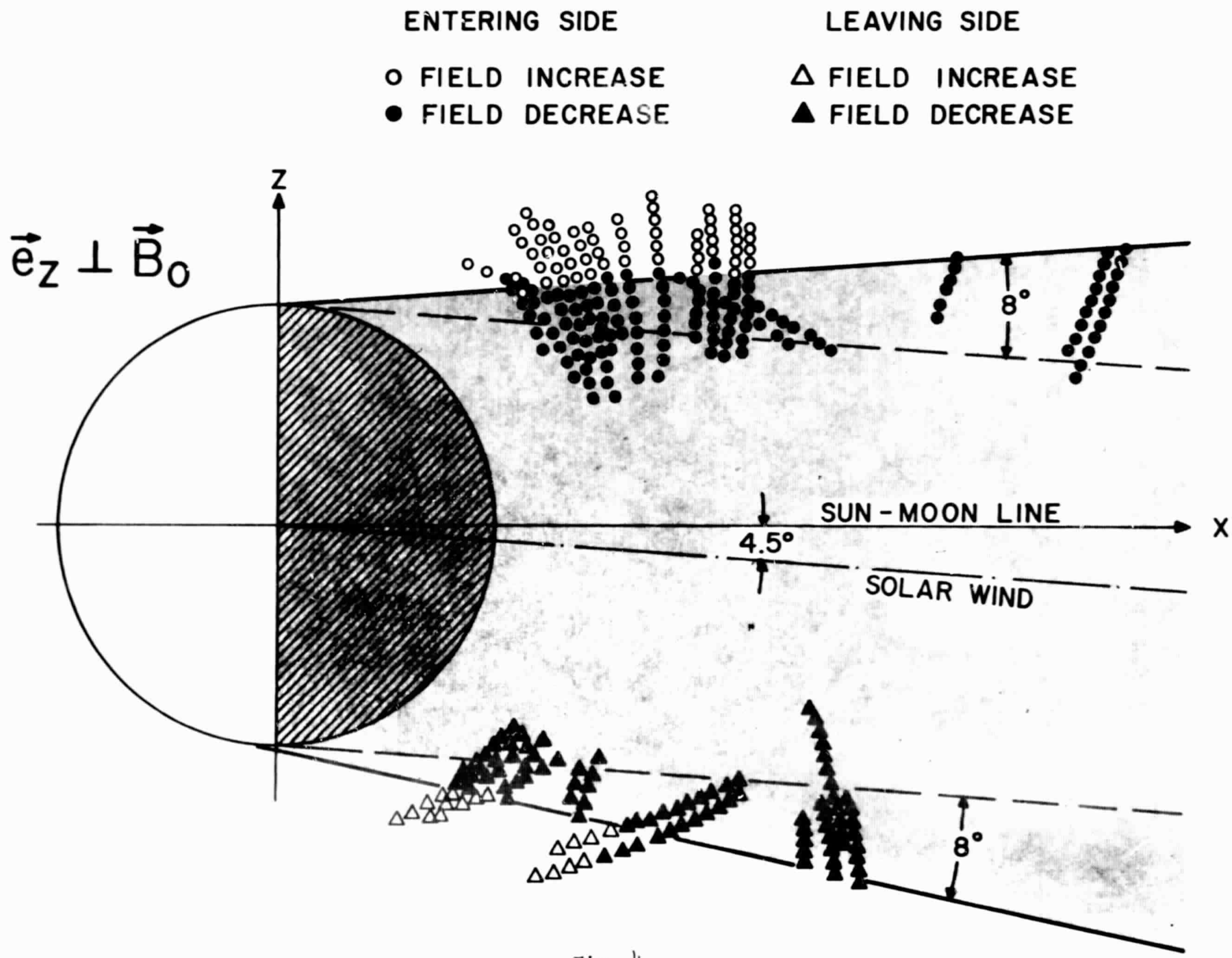
ENTERING SIDE
○ FIELD INCREASE
● FIELD DECREASE
LEAVING SIDE
△ FIELD INCREASE
▲ FIELD DECREASE
$\vec{e}_Z \perp \vec{B}_0$
Z
X
8°
SUN-MOON LINE
4.5°
SOLAR WIND
8°

Fig. 4

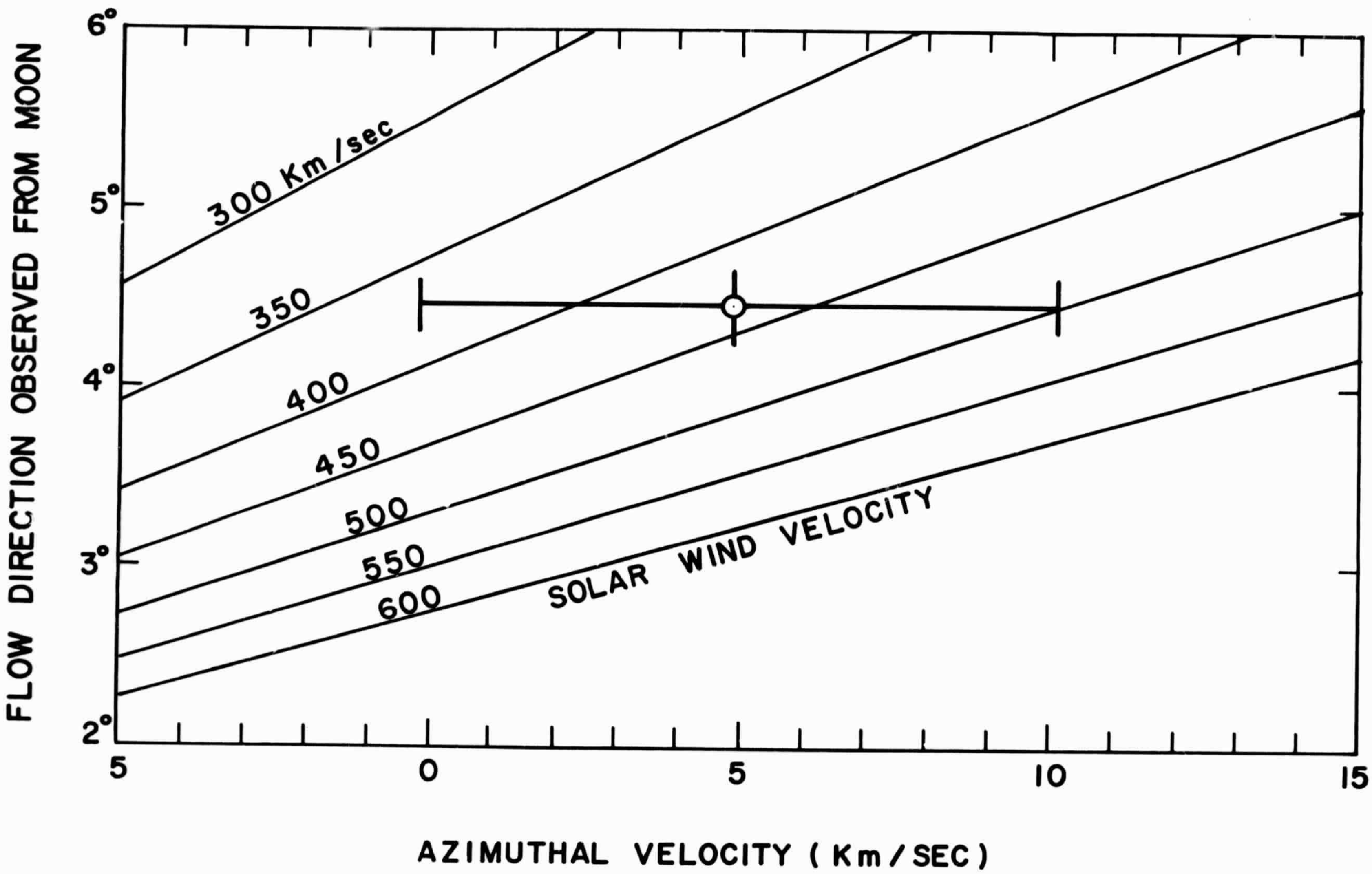
FLOW DIRECTION OBSERVED FROM MOON
6°
5°
4°
3°
2°
300 Km /sec
350
400
450
500
550
600
SOLAR WIND VELOCITY
5
0
5
10
15
AZIMUTHAL VELOCITY (Km / SEC)

Fig. 5

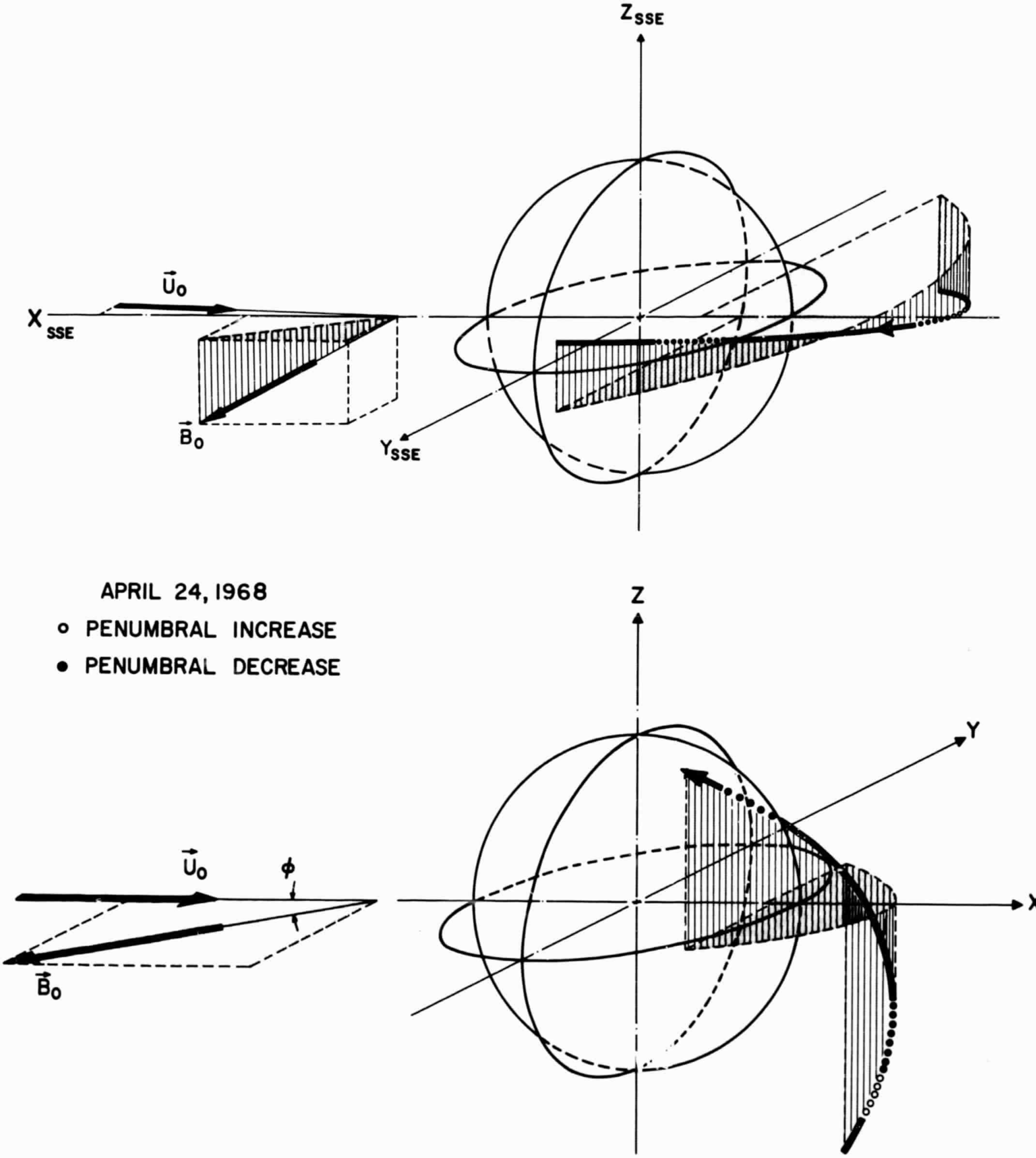
Z_SSE
U_0
X_SSE
B_0
Y_SSE
APRIL 24, 1968
o PENUMBRAL INCREASE
• PENUMBRAL DECREASE
Z
Y
U_0
φ
B_0
X

Fig. 6

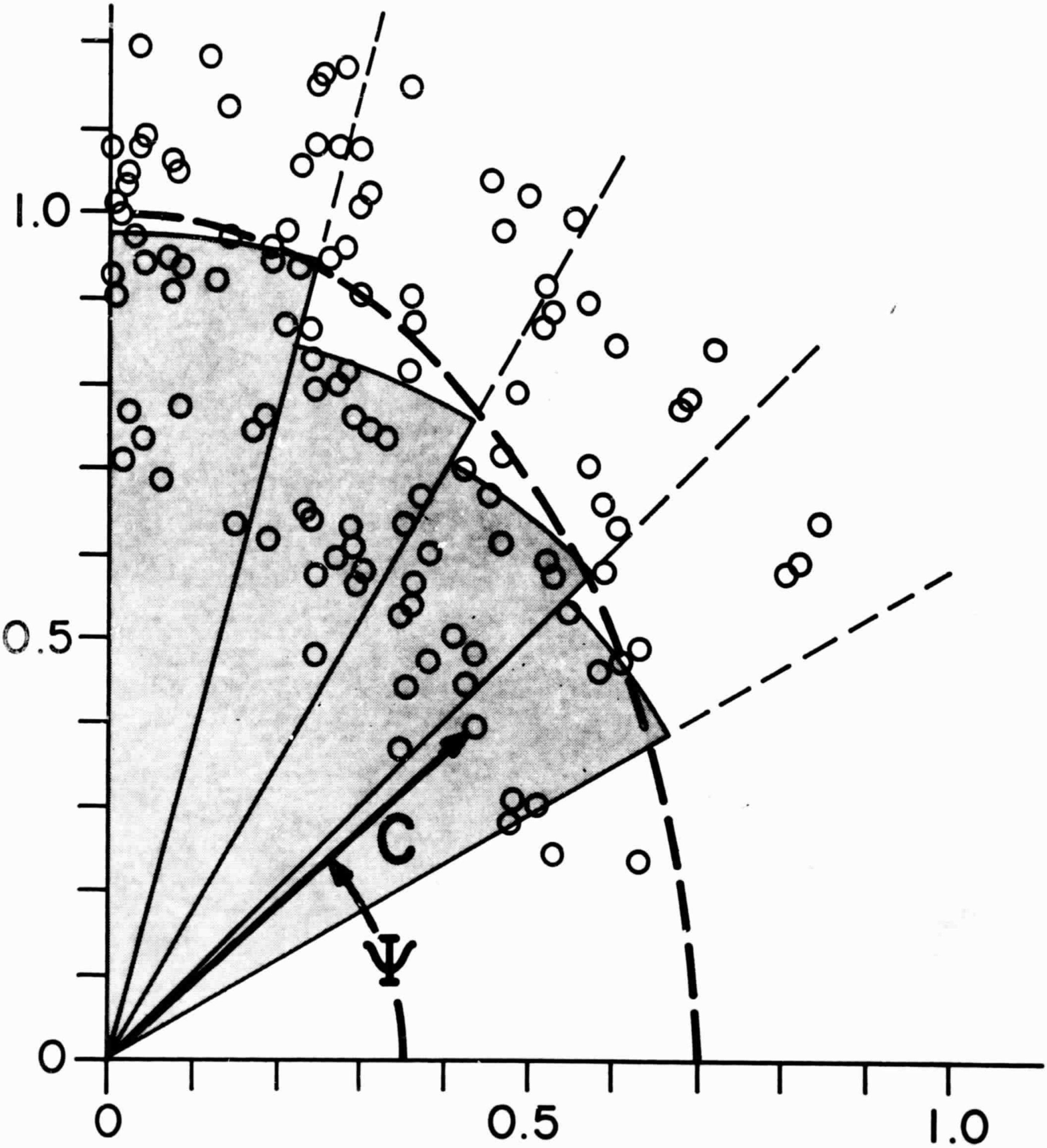

Fig. 7